Ocean Dynamics (2023) 73:23–34
https://doi.org/10.1007/s10236-022-01536-6

Sea level acceleration and variability in the Chesapeake Bay: past trends, future projections, and spatial variations within the Bay

Tal Ezer[1]

Received: 22 August 2022 / Accepted: 15 December 2022 / Published online: 27 December 2022

Abstract

Fast sea level rise (SLR) is causing a growing risk of flooding to coastal communities around the Chesapeake Bay (hereafter, CB or "the Bay"), but there are also significant differences in sea level variability and sea level rise rates within the bay that have not been fully investigated in the past. Therefore, monthly sea level records for 1975–2021 from eight tide gauge stations, from the upper bay at Baltimore, MD, to the lower bay at Norfolk, VA, are analyzed and compared. The results show significant spatial variations within the Bay over a wide range of time scales. The largest contribution to the seasonal variations of mean sea level in the Bay is from the annual (S_A) and semiannual (S_{SA}) tides, while the contribution from thermosteric changes is relatively smaller. The lower Bay has a ~5 cm smaller mean annual sea level range than the upper Bay and has a secondary minimum in mid-year due to a larger semiannual tide than the upper Bay which is dominated by the annual tide. Variations in sea level anomaly (after removing the mean seasonal cycle) show anticorrelation between the upper and lower bay. Empirical mode decomposition (EMD) analysis reveals that variations with opposite phases at the two edges of the Bay appear mostly on decadal time scales that are linked with the North Atlantic Oscillation (NAO). Sea level trends vary along the Bay—linear SLR rates (4.5–6.1 mm y^{-1}) increase from north to south, while sea level acceleration rates (all positive in the range 0.012–0.16 mm y^{-2}) increase from south to north. The linear SLR pattern is driven by land subsidence rates, while the acceleration pattern suggests potential impacts from climate change signals that enter the mouth of the Bay in the southeast and amplified farther north by local dynamics. Monthly sea level projections until 2100, based on past trends and the seasonal cycle of each station, are compared with different SLR scenarios based on climate models. The results suggest that accounting for local sea level acceleration in projections can result in large differences in local future sea level rise.

Keywords Chesapeake Bay · Sea level rise · Tides · Seasonal variations

1 Introduction

Sea level rise is causing a major risk for many coastal regions worldwide that see an increase in frequency and severity of flooding (Nicholls and Cazenave 2010; Cazenave and Le Cozannet 2014; Buchanan et al. 2017; Taherkhani et al. 2020). The U.S. East Coast is especially vulnerable to increased flooding (Ezer and Atkinson 2014; Sweet and Park 2014; Sweet et al. 2017, 2018, 2022; Ezer 2022); the impact of flooding is already evident from South Florida (Wdowinski, et al. 2016; Valle-Levinson et al. 2017; Domingues et al. 2018; Alarcon et al. 2022) to Boston (Kruel 2016). In addition to global sea level rise (Kopp et al. 2014, 2017; Dangendorf et al. 2019), local sea level rise and flooding along the U.S. East Coast are affected by a combination of various other factors, including land subsidence (Boon et al. 2010; Eggleston and Pope 2013; Bekaert et al. 2017; Buzzanga et al. 2020), changes in tidal range (Cheng et al. 2017; Lee et al. 2017), storm surge due to hurricanes and tropical storms (Ezer et al. 2017; Knutson et al. 2019; Ezer 2020b; Park et al. 2022), and changes in ocean circulation such as potential weakening of the Atlantic Meridional Overturning Circulation, AMOC (Ezer 2015), and the Gulf Stream (Ezer et al. 2013; Park and Sweet 2015). Decadal variations in

Responsible Editor: Jia Wang

This article is part of the Topical Collection on the *12th International Workshop on Modeling the Ocean (IWMO), Ann Arbor, USA, 25 June – 1 July 2022*

✉ Tal Ezer
tezer@odu.edu

[1] Center for Coastal Physical Oceanography, Old Dominion University, 4111 Monarch Way, Norfolk, VA 23508, USA

AMOC (Latif et al. 2019) may also affect coastal estuaries like the CB.

One region within the U.S. East Coast that emphasizes the high risk from sea level rise is the area around the Chesapeake Bay (CB) and especially its southern region (often refers to as the “Tidewater” or the “Hampton Roads” region) with its high rates of land subsidence (Eggleston and Pope 2013) that results in local SLR that is 2–3 times faster than global SLR (Boon et al. 2010; Ezer 2013). The CB is the largest estuary in the U.S.A. (~280 km long, stretching from southeastern Virginia to northeastern Maryland) with a population of ~18 million people living in the CB watershed and affected by the regional climate change and sea level rise (Boesch et al. 2018). Most of the past studies that focused on analyzing sea level from tide gauges in the CB used data from over a decade ago (e.g., Boon et al. 2010; Boon 2012; Ezer and Corlett 2012); they indicate SLR rates in the CB of ~3–5 mm y^{-1} and typical acceleration of 0.02–0.1 mm y^{-2}. These studies found sea level acceleration like sea level acceleration in other locations in the Mid-Atlantic Bight (MAB) (Boon 2012; Sallenger et al. 2012; Ezer 2013) and consistent with findings of global sea level acceleration in the twentieth century (Church and White 2006), that is most pronounced since the 1960s (Dangendorf et al. 2019). There are however periods of a few years with larger than normal sea level acceleration in the MAB that coincide with periods of weakening in the Gulf Stream flow (Ezer et al. 2013). The large regional SLR in the MAB from 1950 to 2009 was referred to as “hotspot” (Sallenger et al. 2012). However, recent observations suggest that over the last decade or so this “hotspot” of large SLR had shifted to the South Atlantic Bight (Valle-Levinson et al. 2017; Domingues et al. 2018; Ezer 2019). Moreover, decadal climate variations as well as the 18.6-year nodal tidal cycle (Baart et al. 2011; Haigh et al. 2011) may change local SLR rates and acceleration from decade to decade.

The goal of this study is to revisit sea level data in the CB using more recent data (until December 2021) and examine the SLR and acceleration rates to assess whether or not sea level rise continues its acceleration in the CB despite the recent shift of the hotspot to southern U.S. coasts. A particular focus of the study is on potential differences between locations within the Bay and examining spatial variations in sea level to find what factors can cause differences in sea level between the upper and lower Bay. Monthly sea level data since 1975 are used to allow comparisons between stations (in contrast, some past studies such as Ezer and Corlett 2012 or Boon 2012 used different record lengths for different stations in the CB). Variations in sea level are investigated over a wide range of time scales from seasonal and interannual variability to decadal oscillations and long-term trends.

Future projections of sea level rise are essential to allow planning of mitigation and adaptation to sea level rise. However, projections from global climate models may neglect local variations and local dynamics, so another goal of the study is to compare projections based on variability and trends of past data (e.g., Boon 2012) with projections based on climate models (e.g., Kopp et al. 2014, 2017; Parris et al. 2012).

The study is organized as follows. First, the data sources and methods are described in Section 2, then results are presented in Section 3, first for variations in past sea level and then for projection of future sea level, finally, a summary and conclusions are offered in Section 4.

2 Data sources and methods

Monthly water level records for CB were obtained from NOAA (https://tidesandcurrents.noaa.gov/). The period 1975–2021 (47 years) was chosen for the analysis, to allow comparison between eight tide gauge stations with continuous records, from Baltimore in the north to Norfolk in the south (Fig. 1). Note that 5 stations are located on the western shore of the CB, 2 stations on the eastern shore and one station, CBBT, is located on an artificial man-made island to support a bridge, so that geology-based land dynamics, like subsidence, can be different in different locations, as shown later. Small gaps in data were filled by interpolation. It is well known that land subsidence varies along the CB and affects local SLR (Boon et al. 2010; Eggleston and Pope 2013; Bekaert et al. 2017). Since geological time scales of vertical land movement are very long it is assumed that subsidence contributes mostly to linear local SLR rates, though remote sensing data show large small-scale variations in vertical land movement that are not fully explained (Buzzanga et al. 2020). Nonlinear SLR variations such as sea level acceleration (ACC) in the Bay (Ezer and Corlett 2012) can be driven by oceanic and atmospheric dynamic processes such as wind, air pressure, or variations in the Gulf Stream (Ezer et al. 2013).

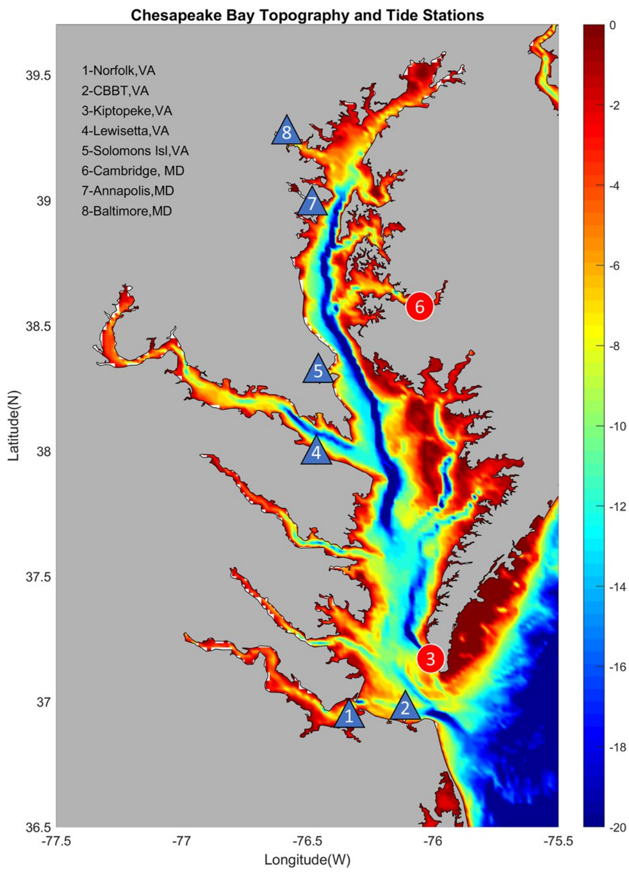

Fig. 1 A topographic map (depth in meters) of the Chesapeake Bay and locations of tide gauge stations. Stations on the southern and western shores of CB are marked by blue triangles and stations on the eastern shore by red circles

Therefore, to study the linear and nonlinear (i.e., acceleration) trends, polynomial regression fit was used, assuming that sea level can be represented by

$$\eta(t)=at^2+bt+c. \tag{1}$$

Linear regression (with $a=0$) will provide SLR = b (in mm y^{-1}) and quadratic regression will provide acceleration ACC $=\partial^2{}_\eta/\partial t^2=2a$ (in mm y^{-2}).

To estimate the contribution of long astronomical tides to the seasonal cycle of sea level, the harmonic tidal constituents of the annual (S_A) and semiannual (S_{SA}) tides were obtained for tide gauge stations from NOAA's Tides and Currents site. The relative sea level associated with these long tidal cycles can then be estimated by

$$\eta(t) = A_{SA}\sin\left(\frac{t}{T_{SA}} - P_{SA}\right) + A_{SSA}\sin\left(\frac{t}{T_{SSA}} - P_{SSA}\right) \tag{2}$$

where A_j, T_j, and P_j represent the amplitude, period, and phase, respectively, of the two long tides at each station. Equation 2 was used to calculate the monthly mean contribution.

To estimate the contribution of the seasonal temperature changes to thermosteric sea level, monthly water temperature (T) data near tide stations were obtained from NOAA. Mean salinity (S) at different locations in the CB was estimated by the Maryland Department of Natural Resources (https://eyesonthebay.dnr.maryland.gov/eyesonthebay/). Density, $\rho(T,S)$, for each month at each station was then calculated using the linear equation of state (e.g., Eq. 2.1 in Knauss and Garfield 2017), and assuming the mean depth of $H=10$ m, the steric sea level change can be estimated by

$$\eta_S(t) = -H\left(\frac{[\rho(t)-\rho_0]}{\rho_0}\right) \tag{3}$$

where ρ_o is a reference average density. Note that Eq. 3 was used to obtain a rough estimate of the relative contribution to sea level from the seasonal variations in temperature. The steric sea level at a particular location is likely affected by the surrounding region, not just the depth where stations are located, so for easier comparison between stations, a constant depth is assumed.

Sea level rise projections based on climate models and different scenarios of greenhouse gas emissions were obtained from the US Army Corps of Engineers SLR calculator (https://cwbi-app.sec.usace.army.mil/rccslc/slcc_calc.html), using the NOAA-2017 scenarios (Parris et al. 2012; Sweet et al. 2017); these projections for each station include NOAA's estimated local land subsidence. For comparisons with projections based on past data, 3 projections are used: Intermediate-Low, Intermediate, and Intermediate-High. The probability and contributions for different SLR projections are analyzed in Kopp et al. (2017) and other studies.

Decadal climate variability in the Atlantic Ocean is often captured by the North Atlantic Oscillation Index (NAO) (Hurrell et al. 2003). So the NAO monthly index was obtained from (https://climatedataguide.ucar.edu/climate-data/hurrell-north-atlantic-oscillation-nao-index-pc-based) and compared with variations of sea level in the CB.

To analyze sea level variability on different time scales, the empirical mode decomposition (EMD) method was used (Huang et al. 1998; Wu et al. 2007; Wu and Huang 2009). EMD is a nonstationary nonlinear method that breaks time series records into intrinsic mode functions (IMFs) representing oscillations with time-dependent amplitudes and frequencies, $C_i(t)$, and a long-term trend, $r(t)$. Therefore, the time series is represented by

$$\eta(t) = \sum_{i=1}^{N} C_i(t) + r(t) \tag{4}$$

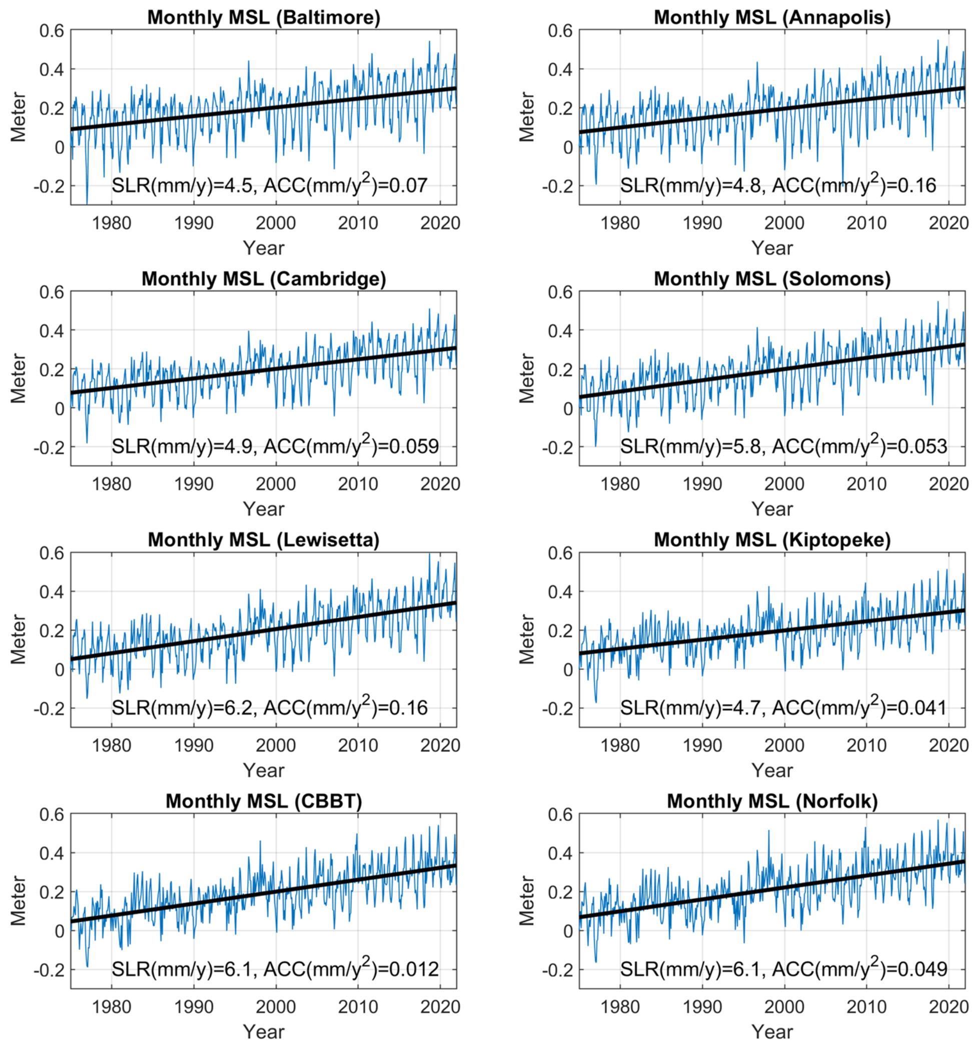

Fig. 2 Monthly mean sea level (blue lines) for the eight stations of Fig. 1, and linear trend (black heavy lines). Mean linear sea level rise rate and acceleration rate over 1975–2021 are listed for each location

where N is the total number of oscillating modes. The EMD method has been used in many studies of sea level variability (Ezer and Corlett 2012; Ezer et al. 2013; Ezer 2015).

3 Results

3.1 Sea level rise and acceleration 1975–2021

Tide gauge stations in the CB have different record lengths—some stations have very long records (e.g., ~120 years in Baltimore, MD, and ~96 years in Sewells Point, Norfolk, VA), but many other stations have much shorter records of few years to few decades (Boon et al. 2010; Boon 2012; Ezer and Corlett 2012; Ezer and Atkinson 2015). Because of interannual and decadal variability, calculating sea level trends over different periods (as is the case if analyzing the entire length of each record) may result in different trends and make it difficult to compare stations. Therefore, here monthly sea level of eight tide gauge stations (Fig. 1) was analyzed over the same period (1975–2021). The analysis (Fig. 2) shows some similarities (e.g., positive anomaly at all stations around 1998), but also differences in rates of SLR and ACC, as well as differences in the seasonal variations (including annual and semiannual cycles, discussed later). During the same period, SLR ranges from 4.5 mm y^{-1} in the upper Bay at Baltimore to 6.1–6.2 mm y^{-1} in the lower Bay at Lewisetta, CBBT, and Norfolk. ACC in coastal stations ranges from 0.041 mm y^{-2} on the eastern shore of the CB in Kiptopeke to 0.16 mm y^{-2} in Annapolis and Lewisetta. One exception is CBBT with the lowest ACC rate of 0.012 mm y^{-2}, but this location is on an artificial island built for holding a bridge, so its dynamics is quite different than the other coastal stations. Estimated errors in the regression are like previous studies (Boon 2012; Ezer and Corlett 2012; Sallenger et al. 2012; Ezer 2013) with SLR ± ~0.2–0.5 mm y^{-1}, ACC ± ~0.01–0.02 mm y^{-2}, and the mean error of the prediction using linear or quadratic fits is ~5–10 cm. The local acceleration is in general consistent with the global

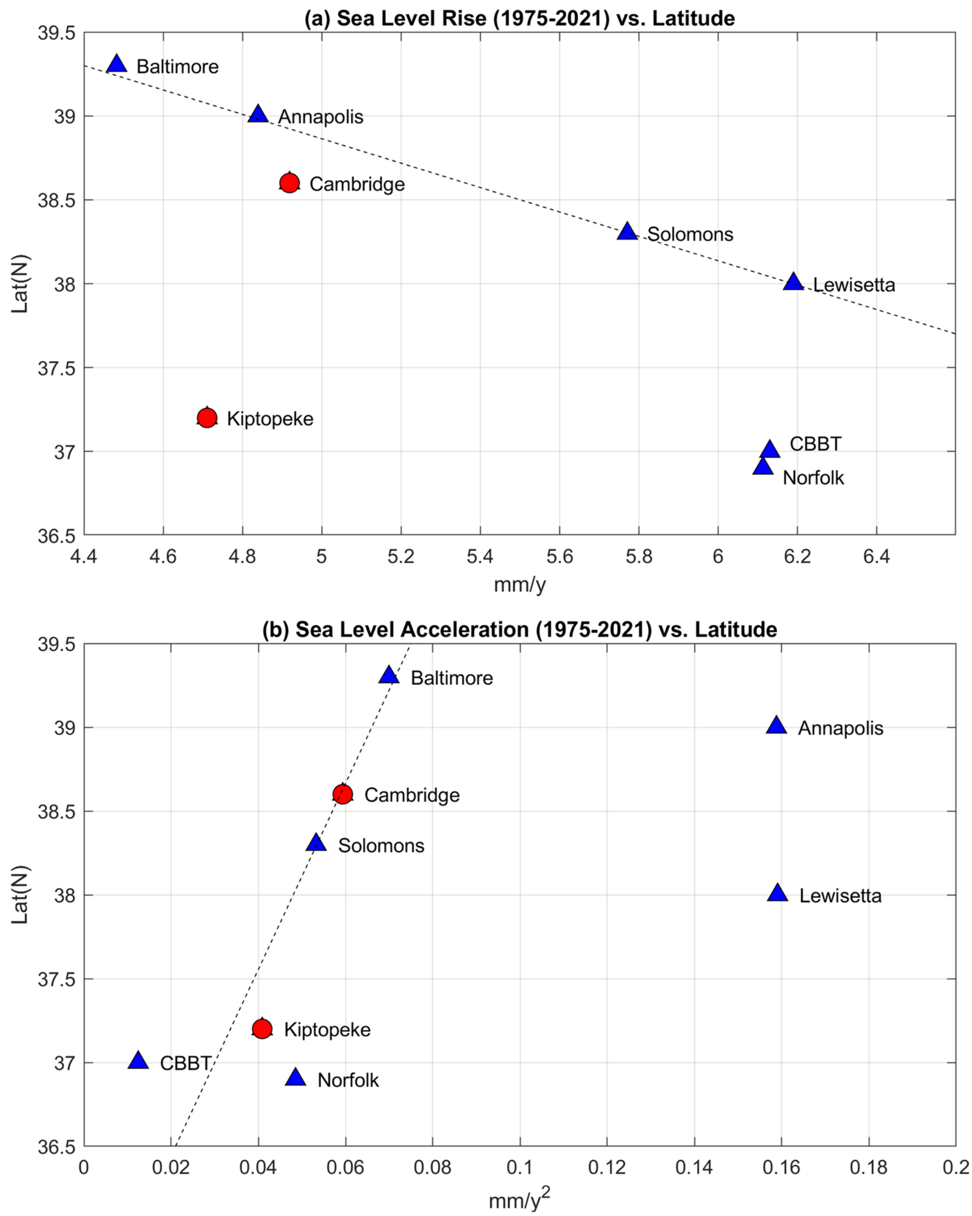

Fig. 3 **a** Linear mean sea level rise rates and **b** mean sea level acceleration rates for 1975–2021, as a function of stations' latitude. Stations on the western shores of the CB are marked by blue triangles and stations on the eastern shores are marked by red circles (as in Fig. 1). Note that the Chesapeake Bay Bridge Tunnel (CBBT) station is located on an artificial island along the bridge. Dash lines highlight stations with values versus latitudes located along the same line

sea level acceleration since 1960, which was in the range of 0.05–0.1 mm y^{-2} (Dangendorf et al. 2019). While the local acceleration is within the global range, the variations of acceleration within the CB are not fully explained and may relate to local dynamics.

The dependency of the SLR and ACC trends on latitude is shown in Fig. 3. SLR shows almost a linear change vs. latitude for five of the eight stations, from Baltimore to Lewisetta (Fig. 3a), which indicates an increase in land subsidence toward the southern part of the Bay. This result is consistent with Karegar et al. (2016) who show almost a linear decrease trend of land subsidence as a function of latitude between 38°N and 44°N along the U.S. East coast and this trend had little change since geological times. This subsidence is due to the glacial isostatic adjustment (GIA) and geological compression associated with the Chesapeake Bay meteor impact crater (Boon et al. 2010; Eggleston and Pope 2013; Bekaert et al. 2017; Buzzanga et al. 2020). However, it is interesting to note that the three southernmost stations show a large difference in SLR between CBBT and Norfolk to Kiptopeke; the latter station is distinctively different than most other locations, as it is located on the eastern shore, not far from the center of the Chesapeake Bay meteor impact crater (Eggleston and Pope 2013). The results indicate that the lower CB area has a land subsidence rate of at least ~2 mm y^{-1} (compared with the upper Bay), which is consistent with recent spaceborne radar measurements (Bekaert et al. 2017; Buzzanga et al. 2020). Sea level acceleration rates (ACC), however, have much different dependency on latitude (Fig. 3b) than SLR rates (Fig. 3a).

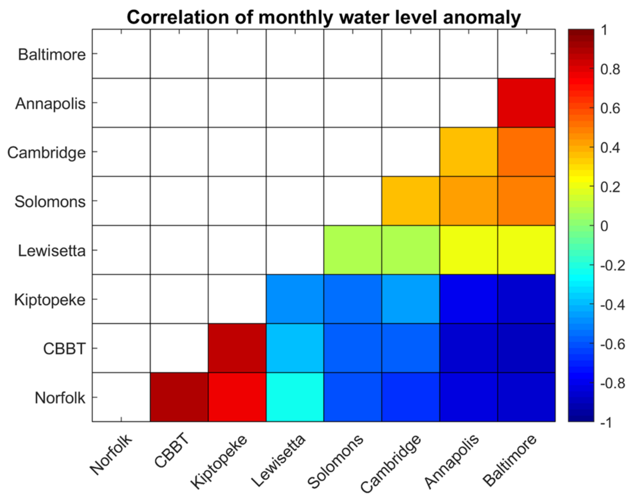

Fig. 4 Correlations of sea level anomaly (relative to the monthly mean of all stations) between the different stations. The stations are arranged from the uppermost station (upper-right corner) to the lowermost station (lower-left corner)

Six of the eight stations sit on a similar line, and two stations, Annapolis and Lewisetta have much larger acceleration that may indicate impacts from local dynamics. It is not clear what factors affect this pattern, but the fact that CBBT has the lowest acceleration, may suggest that dynamic oceanic signals that enter the CB mouth from the Atlantic Ocean are amplified when they move north along the Bay. Note however that unlike the other coastal stations, CBBT station is located on an artificial island along the Chesapeake Bay Bridge Tunnel.

3.2 Variations of sea level anomaly within the CB

The monthly sea level variability (Fig. 2) is dominated by two main factors, the annual (seasonal) cycle and the sea level rise trend. To study the differences between stations, the mean sea level of all 8 stations is subtracted from each individual record, which results in a sea level anomaly that excludes the mean SLR and the mean seasonal cycle of the CB. Calculating correlations of sea level anomaly between all stations (Fig. 4) reveals a distinct pattern: the 3 southern stations (Norfolk to Kiptopeke) and the 5 northern stations (Lewisetta to Baltimore) are positively correlated with each other (yellow to red colors), but the southern and northern stations are negatively correlated (blue color). This pattern indicates a mode of variability with opposite phase between the northern and southern parts of the CB. To further investigate the relation between the sea level in the upper and lower bay, the time series of the upper Bay was defined as the mean of Annapolis and Baltimore and the lower Bay as the mean of Norfolk and Kiptopeke. Then, cross-correlations between EMD modes of the two time series were calculated (Fig. 5). The highest frequency EMD mode (Mode 1; top panel of Fig. 5) indicates a positive correlation $R = 0.6$ at time scales of few months, which is probably associated with the passage of weather systems over the region. Modes 2 and 3 capture the annual cycle, which is coherent (positive correlation with no lag) across the Bay. Modes 4 and 5 capture oscillations at ~3–7 year periods that are still positively correlated across the Bay. However, modes 6 and 7 show negative correlations with oscillations of ~10–20 year periods (lower 2 panels of Fig. 5). In these low-frequency modes, there is also a lag between the lower and upper Bay. Therefore, the anticorrelation seen in Fig. 4 (after removing the annual cycle) between the upper and lower Bay seems to be driven by decadal large-scale variability.

To further investigate the decadal variations, the low-frequency modes (the combined modes 6 and 7 in Fig. 5) are compared with low-frequency modes of the NAO index in Fig. 6. The sea level anomaly in the CB is anti-correlated with the NAO, but the sea level in the lower Bay has much higher correlation ($R = -0.55$; $>95\%$ confidence level) than the upper bay ($R = -0.19$). This result suggests that the decadal variations are in fact driven by the Atlantic Ocean as their signal enters through the mouth of the CB; farther in the upper Bay there may be additional unknown dynamics. The link between NAO and coastal sea level has been shown in many past studies (e.g., Ezer 2019), for example, around 2010 low NAO index and weak AMOC resulted in increased sea level along the entire U.S. East Coast (Ezer 2015; Goddard et al. 2015), as seen also here in Fig. 6.

3.3 The annual cycle of sea level and its causes

The monthly mean sea level calculated as the average of each month over the entire period (Fig. 7) shows 3 distinct patterns for stations in the upper Bay (2 stations), the middle Bay (3 stations), and the lower Bay (3 stations). All stations show maximum sea level in September, but stations in the lower Bay have two minima, one in January and a secondary one in July. Two potential contributors to the annual cycle of sea level are considered, the seasonal temperature variations and the annual and semiannual tides. The temperature record at 3 stations (Fig. 8a) shows a very similar seasonal cycle with maximum temperature in July–August, unlike the sea level that had a maximum in September (Fig. 7). Temperature in the lower Bay (Norfolk) has slightly smaller seasonal range (as sea level does). However, estimating the thermosteric sea level change associated with the seasonal temperature (Eq. 3) reveals a seasonal range of less than 4 cm (Fig. 8b), compared with the observed range of 20–25 cm (Fig. 7), so one must conclude that the contribution of thermal expansion to the seasonal sea level is small (~20% or less).

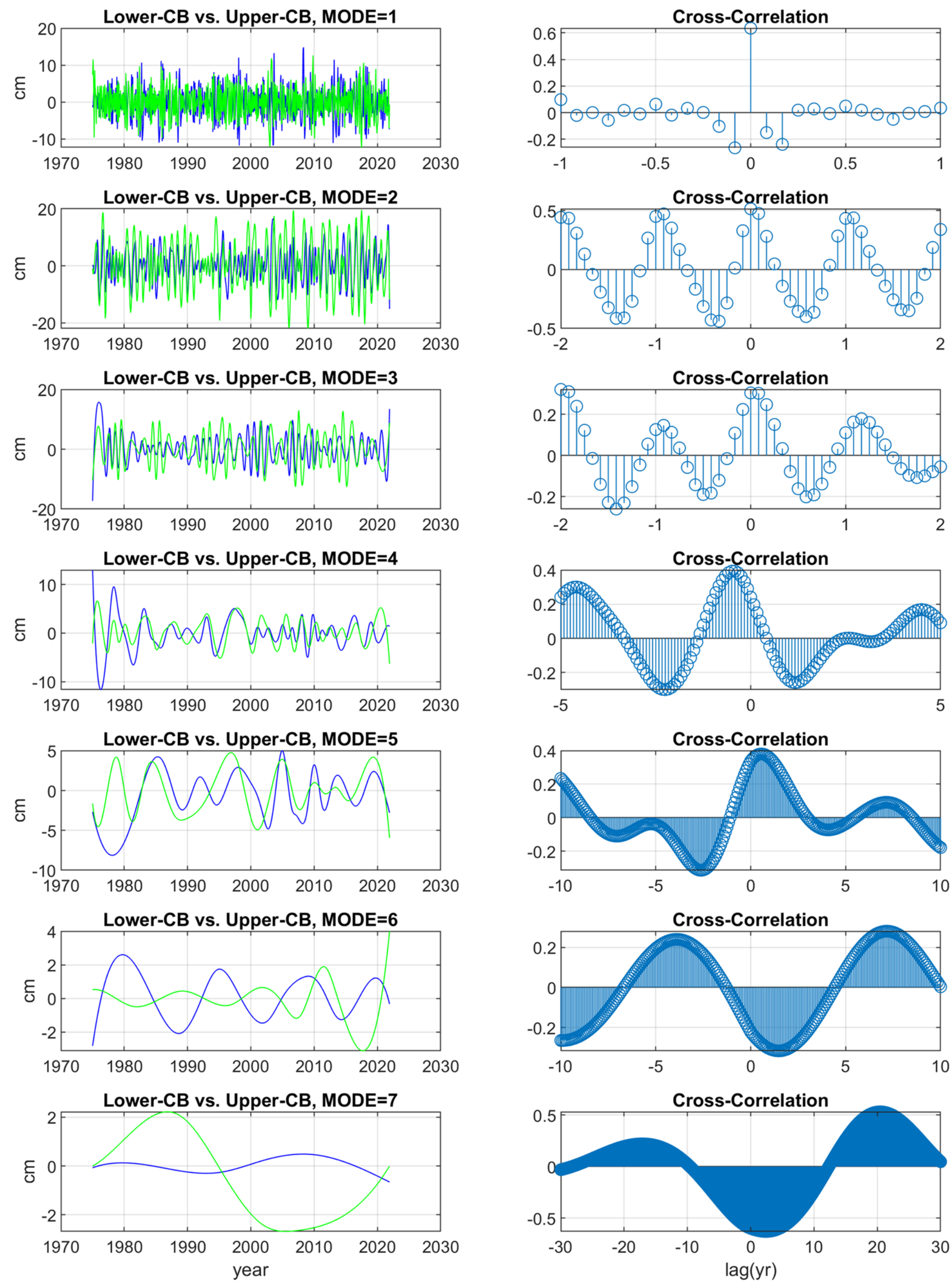

Fig. 5 Left panels: comparison of EMD modes of mean sea level in the lower CB (Norfolk to Kiptopeke; in green) and upper CB (Annapolis and Baltimore; in blue). Right panels: cross correlation; note the different lag scale in each panel

Studies show that the annual and semiannual tides can contribute significantly to seasonal variations in sea level along the U.S. East Coast (Ezer 2020a), so the tidal contribution in Baltimore and Norfolk was estimated from the NOAA's S_A and S_{SA} tidal constituents (Eq. 2) and shown in Fig. 9. This comparison shows two important results: First, that the range of seasonal sea level change due to long-term tides, about 20–25 cm, and the maximum sea level in September is consistent with the observations in Fig. 7. Second, that the differences between the upper Bay (Baltimore) and lower Bay (Norfolk) are consistent with the observations that show that the seasonal sea level in the lower Bay has ~5 cm smaller range than the upper Bay and has a secondary minimum in mid-year (though two months before the observed minimum). The secondary minimum suggests that the lower Bay has more influence from the semiannual tides, and in fact, the relative amplitude of S_{SA}, $A_{SSA}/(A_{SA}+A_{SSA})$ is 0.41 in Norfolk and 0.23 in Baltimore. It is acknowledged though that estimated annual and semiannual tides (Eq. 2) based on NOAA constituents cannot exactly reproduce the observed seasonal sea level (which is affected by many

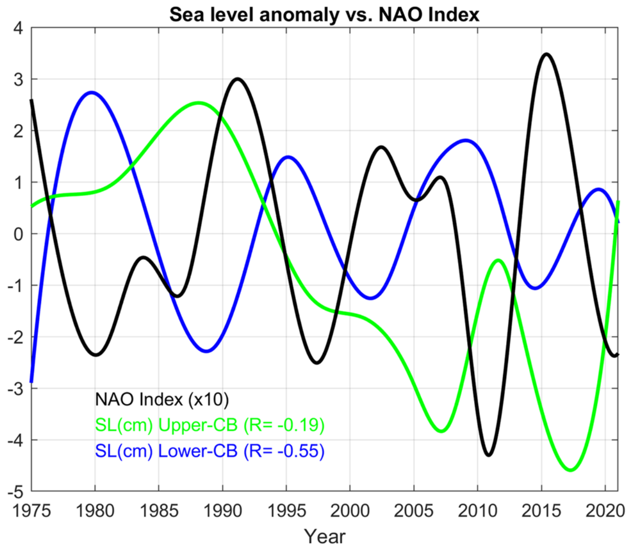

Fig. 6 Correlation between decadal variations of sea level and decadal variations in the NAO Index. The low-frequency modes (EMD modes 6 and 7 in Fig. 5) are shown for the sea level anomaly of the upper CB (green line) and lower CB (blue line) and compared with the low-frequency modes of NAO (also obtained from EMD modes 6 and 7 and shown in black line). Correlations between sea level and NAO are shown

other factors such as seasonal variations in temperature, seasonal wind, and river flow), but they clearly demonstrate that tides are the largest contributors.

3.4 Future projections of sea level rise

Two methods for projections of future sea level rise until 2100 are compared. The first method is based on climate models

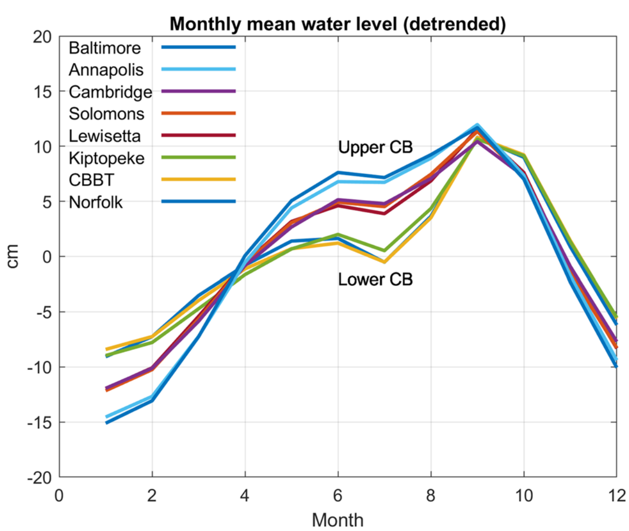

Fig. 7 Monthly mean annual cycle of sea level at the eight stations. Note the three clusters of lower-, middle- and upper-CB

that estimate different scenarios of greenhouse gas emissions and applied by NOAA to tide gauge locations by adding estimates of local vertical land movement (Parris et al. 2012; Sweet et al. 2017). Three of these NOAA projections (intermediate-low, intermediate, and intermediate-high) were obtained for 2000–2100 for 6 locations; the projections were adjusted so the intermediate sea level projection for 2021 will match the observations. The second approach is using only statistics of past sea level trends to project future changes. For example, Boon (2012) used a quadratic fit of sea level variability from 1969–2011 to project sea level rise until 2050; statistics of the variability in the data was used to estimate projection errors. Here, a similar approach is taken, but also adding the seasonal cycle and uncertainty of each location. The mean monthly sea level projection until 2100 at each location is calculated from the quadratic fit (Eq. 1) of the monthly sea level for 1975–2021 (as in Boon 2012). But then the mean annual cycle of the CB was added plus a random sampling of the sea level anomaly at each station. The anomaly represents other unpredictable factors such as storms, precipitation, river flow, and atmospheric pressure, which may be different at different locations and different times (e.g., infrequent hurricanes and tropical storms), therefore the random sampling of past water level should represent the combination of all the unknown factors. The comparison of the two methods is shown in Fig. 10. While the NOAA projections are almost the same for all locations (only small differences in land subsidence vary with locations), the statistic-based projections vary significantly from station to station. The coastal station (excluding CBBT) with the smallest acceleration (of the 6 stations shown in Fig. 10) during 1975–2021, Kiptopeke (Fig. 3b), has statistical projection just above the intermediate-low NOAA projection (Fig. 10e), while the stations with the highest acceleration, Annapolis and Lewisetta (Fig. 3b) have projections for 2100 between the intermediate and intermediate-high NOAA projections (Fig. 10b, d). Projections of most stations fall between the intermediate-low and the intermediate NOAA projections. It is unknown which projection method is more accurate, and many factors in the climate system may change in the next 80 years, however, the results demonstrate that based on past statistics alone, variations in local acceleration may cause as much as 0.5 m difference in 2100 sea level projection for different locations. Local dynamic adjustment is likely to prevent such large variations within the CB, but to assess dynamic processes in the Bay due to spatial variations will need help from numerical ocean modeling, which is beyond the scope of this study.

4 Summary and discussion

The Chesapeake Bay is the largest estuary in the U.S.A., with important wetland ecosystems and a large population along its shores that are affected by climate change. The

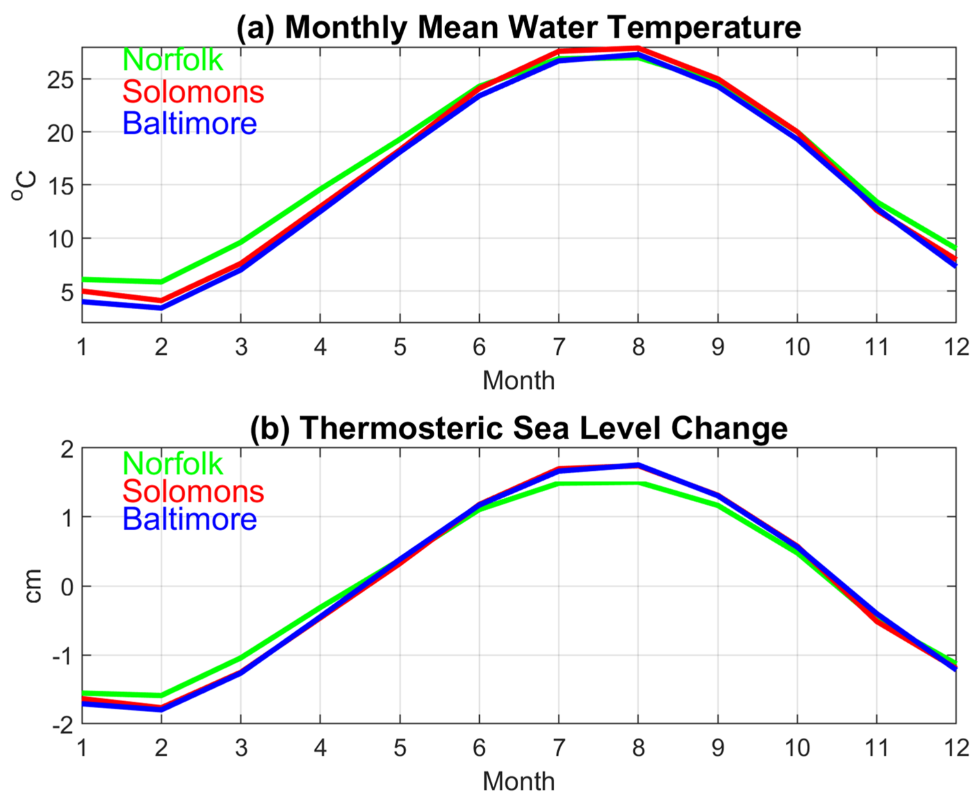

Fig. 8 **a** Monthly mean annual cycle of surface water temperature at three stations. **b** Estimated monthly sea level change due to the thermosteric effect, using linear density equation, typical salinity for each location, and constant depth of 10 m

increased frequency of flooding due to fast sea level rise (Ezer and Atkinson 2014, 2015; Boesch et al. 2018; Sweet and Park 2014; Sweet et al. 2017, 2018, 2022) put many communities at risk. Local sea level rise is faster in the region due to land subsidence (Boon et al. 2010; Eggleston and Pope 2013; Bekaert et al. 2017; Buzzanga et al. 2020) and the potential slowdown of the Gulf Stream (Ezer et al. 2013). The above facts are well known; however, most past studies that focused specifically on sea level rise from tide gauges in the CB (Boon et al. 2010; Boon 2012; Ezer and Corlett 2012) used data from at least a decade ago. Since SLR rates change over time it is important to revisit the CB sea level issue using more recent data (until 2021). Moreover, past studies did not pay much attention to explain variations within the Bay and the mechanisms involved, so here, data from eight tide gauges are compared over the same period of almost 5 decades (1975–2021).

Some of the interesting findings about spatial variations within the bay includes the following:

1. A significant annual cycle of mean sea level (~20–25 cm range) in the Bay is largely due to the annual (S_A) and semiannual (S_{SA}) tides; the upper Bay is dominated by S_A while a more significant contribution from S_{SA} is seen in the lower Bay. This annual pattern of sea level can cause more flooding in the fall (the so called "King Tide" event; Loftis et al. 2019; Hutton and Allen 2021).
2. The seasonal variations in temperature have only minor contributions to the annual mean sea level cycle (~20%) and have only small variations within the Bay; this is different from seasonal steric sea level variations in the open ocean (e.g., Thomson and Tabata 1987).

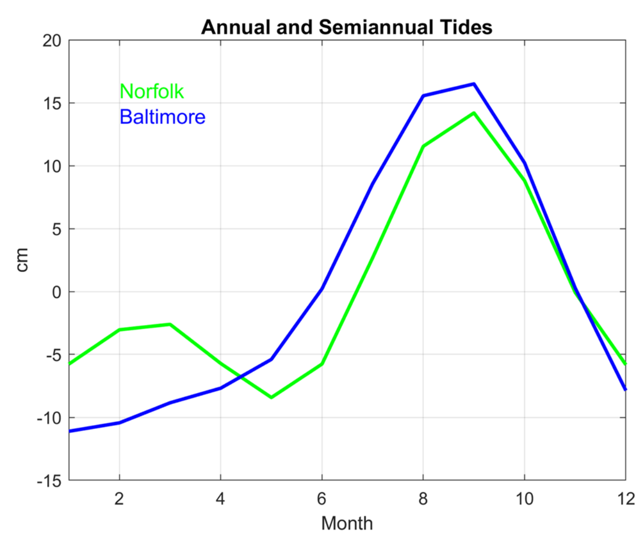

Fig. 9 Estimated monthly mean sea level change due to the annual (S_A) and semiannual (S_{SA}) tides, using NOAA's tidal constituents for Baltimore (blue) and Norfolk (green)

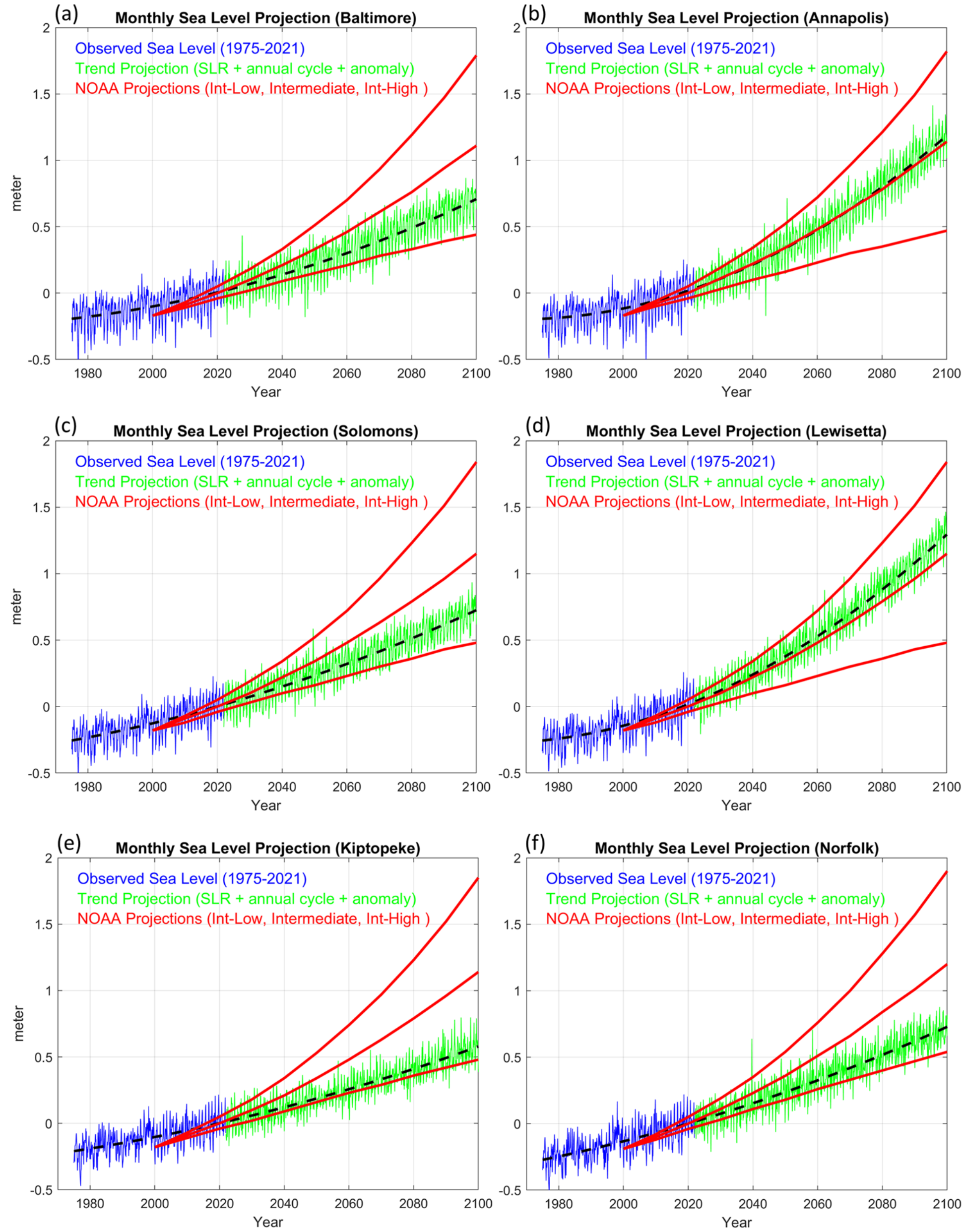

Fig. 10 Past (1975–2021; blue) and future (2022–2100; green) monthly sea level at six locations. The projection is based on a quadratic fit to past data (dash black line) plus the annual cycle and variability at each location. The projection based on past trends is compared with NOAA's projections (red lines) for 3 SLR scenarios, Intermediate-Low, Intermediate, and Intermediate-High. The NOAA projections for 2000–2100 are based on global climate models and local vertical land movement; reference level was adjusted to fit the observed sea level in 2020

3. Sea level anomaly relative to the mean annual cycle shows a mode with an opposite phase between the upper and lower Bay and this mode is likely driven by large-scale decadal variability that is linked with decadal variability of the NAO.
4. Linear SLR increases from north to south due to increased land subsidence in the southern Bay (with exception of the eastern shore), but sea level acceleration generally increases from south to north. The latter suggests that acceleration is affected by potential long-term climate change signals in the Atlantic Ocean which enter the mouth of the Bay in the south and are amplified farther north.
5. Sea level projections until 2100 that combine past trends, seasonal variations, and other unpredictable factors were compared with NOAA projections based on climate models. The results demonstrate that projections based on past observations can vary significantly within the Bay due to differences in sea level acceleration at different locations.

The study helps to better understand recent spatial and temporal sea level variability on a wide range of time scales and the challenge of projecting future sea rise, even within the same estuary. Such studies are useful for planning mitigation and adaptation options for the region at high risk of increased flooding.

Acknowledgements The research is part of ODU's Institute for Coastal Adaptation and Resilience (ICAR). The Center for Coastal Physical Oceanography (CCPO) provided computational support. Special recognition is given to Larry Atkinson (1941-2020) whose pioneering research on the Chesapeake Bay and sea level rise lead the way for many studies including this one.

Data availability The monthly tide gauge sea level record as well as the tidal constituents used here are available from NOAA's Tides and Currents site (https://tidesandcurrents.noaa.gov/). The NOAA's sea level projections were obtained from the USACE website (https://cwbi-app.sec.usace.army.mil/rccslc/slcc_calc.html). The NAO Index was obtained from UCAR (https://climatedataguide.ucar.edu/climate-data/hurrell-north-atlantic-oscillation-nao-index-pc-based). All data are available from the links provided in the paper.

Declarations

Conflict of interest The author declares no competing interests.

References

Alarcon VJ, Linhoss AC, Kelble CR, Mickle PF, Sanchez-Banda GF, Mardonez-Meza FE, Bishop J, Ashby SL (2022) Coastal inundation under concurrent mean and extreme sea-level rise in Coral Gables, Florida, USA. Nat Haz 111:2933–2962. https://doi.org/10.1007/s11069-021-05163-0

Baart F, van Gelder PH, de Ronde J, van Koningsveld M, Wouters B (2011) The effect of the 18.6-year lunar nodal cycle on regional sea-level rise estimates. J Coastal Res 28(2):511–516. https://doi.org/10.2112/JCOASTRES-D-11-00169.1

Bekaert DPS, Hamlington BD, Buzzanga B, Jones CE (2017) Spaceborne synthetic aperture radar survey of subsidence in Hampton Roads, Virginia (USA). Sci Rep 7:14752. https://doi.org/10.1038/s41598-017-15309-5

Boesch DF, Boicourt WC, Cullather RI, Ezer T, Galloway GE, Johnson ZP, Kilbourne KH, Kirwan ML, Kopp RE, Land S, Li M, Nardin W, Sommerfield CK, Sweet WV (2018) Sea-level rise projections for Maryland, University of Maryland Center for Environmental Science, Cambridge, MD, 28 pp. https://www.umces.edu/sea-level-rise-projections

Boon JD (2012) Evidence of sea level acceleration at U.S. and Canadian tide stations, Atlantic coast, North America. J Coast Res 28(6):1437–1445. https://doi.org/10.2112/JCOASTRES-D-12-00102.1

Boon JD, Brubaker JM, Forrest DR (2010) Chesapeake Bay land subsidence and sea level change: an evaluation of past and present trends and future outlook. Special report in applied marine science and ocean engineering, 425, Virginia Institute of Marine Science. https://doi.org/10.21220/V58X4P

Buchanan MK, Oppenheimer M, Kopp RE (2017) Amplification of flood frequencies with local sea level rise and emerging flood regimes. Environ Res Lett 12(6):064009. https://doi.org/10.1088/1748-9326/aa6cb3

Buzzanga B, Bekaert DPS, Hamlington BD, Sangha SS (2020) Toward sustained monitoring of subsidence at the coast using InSAR and GPS: an application in Hampton Roads, Virginia. Geophys Res Lett 47(18): e2020GL090013. https://doi.org/10.1029/2020GL090013

Cazenave A, Le Cozannet G (2014) Sea level rise and its coastal impacts. Earth's Future 2(2):15–34. https://doi.org/10.1002/2013EF000188

Cheng Y, Ezer T, Atkinson LP (2017) Analysis of tidal amplitude changes using the EMD method. Cont Shelf Res 148:44–52. https://doi.org/10.1016/j.csr.2017.09.009

Church JA, White NJ (2006) A 20th century acceleration in global sea-level rise. Geophys Res Lett 33(1). https://doi.org/10.1029/2005GL024826

Dangendorf S, Hay C, Calafat FM, Marcos M, Piecuch CG, Berk K, Jensen J (2019) Persistent acceleration in global sea-level rise since the 1960s. Nat Clim Chan 9:705–710. https://doi.org/10.1038/s41558-019-0531-8

Domingues R, Goni G, Baringer M, Volkov D (2018) What caused the accelerated sea level changes along the U.S. East Coast during 2010–2015? Geophy Res Lett 45(24):13,367–13,376. https://doi.org/10.1029/2018GL081183

Eggleston J, Pope J (2013) Land subsidence and relative sea-level rise in the southern Chesapeake Bay region. U.S. Geological Survey Circular 1392. https://doi.org/10.3133/cir1392

Ezer, T. (2013). Sea level rise, spatially uneven and temporally unsteady: Why the U.S. East Coast, the global tide gauge record and the global altimeter data show different trends. Geophys Res Lett 40(20):5439–5444. https://doi.org/10.1002/2013GL057952

Ezer T (2015) Detecting changes in the transport of the Gulf Stream and the Atlantic overturning circulation from coastal sea level data: the extreme decline in 2009–2010 and estimated variations for 1935–2012. Glob Planet Change 129:23–36. https://doi.org/10.1016/j.gloplacha.2015.03.002

Ezer T (2019) Regional differences in sea level rise between the Mid-Atlantic Bight and the South Atlantic Bight: is the Gulf Stream to blame? Earth's Future 7(7):771–783. https://doi.org/10.1029/2019EF001174

Ezer T (2020a) Analysis of the changing patterns of seasonal flooding along the U.S. East Coast. Ocean Dyn 70(2):241–255. https://doi.org/10.1007/s10236-019-01326-7

Ezer T (2020b) The long-term and far-reaching impact of hurricane Dorian (2019) on the Gulf Stream and the coast. J Mar Syst 208. https://doi.org/10.1016/j.jmarsys.2020b.103370

Ezer T (2022) A demonstration of a simple methodology of flood prediction for a coastal city under threat of sea level rise: the case of Norfolk, VA, USA. Earth's Future 10(9). https://doi.org/10.1029/2022EF002786

Ezer T, Atkinson LP (2014) Accelerated flooding along the U.S. East Coast: on the impact of sea-level rise, tides, storms, the Gulf Stream, and the North Atlantic Oscillations. Earth's Future 2(8):362–382. https://doi.org/10.1002/2014EF000252

Ezer T, Atkinson LP (2015) Sea level rise in Virginia- causes, effects and response. Virginia Journal of Science 66(3):355–369, Publication of the Virginia Academy of Science. https://doi.org/10.25778/8w61-qe76

Ezer T, Corlett WB (2012) Is sea level rise accelerating in the Chesapeake Bay? A demonstration of a novel new approach for analyzing sea level data. Geophys Res Lett 39(19):L19605. https://doi.org/10.1029/2012GL053435

Ezer T, Atkinson LP, Corlett WB, Blanco JL (2013) Gulf Stream's induced sea level rise and variability along the U.S. mid-Atlantic coast. J Geophys Res 118(2):685–697. https://doi.org/10.1002/jgrc.20091

Ezer T, Atkinson LP, Tuleya R (2017) Observations and operational model simulations reveal the impact of Hurricane Matthew (2016) on the Gulf Stream and coastal sea level. Dyn Atmos Oceans 80:124–138. https://doi.org/10.1016/j.dynatmoce.2017.10.006

Goddard PB, Yin J, Griffies SM, Zhang S (2015) An extreme event of sea-level rise along the Northeast coast of North America in 2009–2010. Nat Commun. https://doi.org/10.1038/ncomms7346

Haigh ID, Eliot M, Pattiaratchi C (2011) Global influences of the 18.61 year nodal cycle and 8.85 year cycle of lunar perigee on high tidal

levels. J Geophys Res 116(C6):C06025. https://doi.org/10.1029/2010JC006645
Huang NE, Shen Z, Long SR, Wu MC, Shih EH, Zheng Q, Tung CC, Liu HH (1998) The empirical mode decomposition and the Hilbert spectrum for non stationary time series analysis. Proc R Soc London Ser A 45:903–995. https://doi.org/10.1098/rspa.1998.0193
Hurrell JW, Kushnir Y, Ottersen G, Visbeck M (eds) (2003) The North Atlantic Oscillation: climate significance and environmental Impact. Geophys Monogr Ser vol 134. AGU, Washington, D. C
Hutton NS, Allen TR (2021) Perceptions of visual and in situ representations of sea level rise and tidal flooding: the blue line project, Norfolk, Virginia. GeoJournal 87:2081–2099. https://doi.org/10.1007/s10708-020-10356-4
Karegar MA, Dixon TH, Engelhart SE (2016) Subsidence along the Atlantic Coast of North America: insights from GPS and late Holocene relative sea level data. Geophys Res Lett 43:3126–3133. https://doi.org/10.1002/2016GL068015
Knauss JA, Garfield NG (2017) Introduction to Physical Oceanography, 3rd edn. Waveland Press, Long Grove, IL, p 310
Knutson TR, Camargo SJ, Chan JCL, Emanuel K, Ho C-H, Kossin J, Mohapatra M, Satoh M, Sugi M, Walsh K, Wu L (2019) Tropical cyclones and climate change assessment: Part II. Projected response to anthropogenic warming. Bull Am Meteorol Soc 101(3):303–322. https://doi.org/10.1175/BAMS-D-18-0194.1
Kopp RE, Horton RM, Little CM, Mitrovica JX, Oppenheimer M, Rasmussen DJ, Strauss BH, Tebaldi C (2014) Probabilistic 21st and 22nd century sea-level projections at a global network of tide-gauge sites. Earth's Future 2:383–406. https://doi.org/10.1002/2014EF000239
Kopp RE, DeConto RM, Bader DA, Hay CC, Horton RM, Kulp S, Oppenheimer M, Pollard D, Strauss BH (2017) Evolving understanding of Antarctic ice-sheet physics and ambiguity in probabilistic sea-level projections. Earth's Future 5:1217–1233. https://doi.org/10.1002/2017EF000663
Kruel S (2016) The impacts of sea-level rise on tidal flooding in Boston Massachusetts. J Coast Res 32(6):1302–1309. https://doi.org/10.2112/JCOASTRES-D-15-00100.1
Latif M, Park T, Park W (2019) Decadal Atlantic meridional overturning circulation slowing events in a climate model. Clim Dyn 53:1111–1124. https://doi.org/10.1007/s00382-019-04772-7
Lee SB, Li M, Zhang F (2017) Impact of sea level rise on tidal range in Chesapeake and Delaware Bays. J Geophys Res 122(5):3917–3938. https://doi.org/10.1002/2016JC012597
Loftis JD, Mitchell M, Schatt D, Forrest DR, Wang HV, Mayfield D, Stiles WA (2019) Validating an operational flood forecast model using citizen science in Hampton Roads, VA, USA. J Mar Sci Eng 7(8):242. https://doi.org/10.3390/jmse7080242
Nicholls RJ, Cazenave A (2010) Sea-level rise and its impact on coastal zones. Science 328:1517–1520. https://doi.org/10.1126/science.1185782
Park J, Sweet W (2015) Accelerated sea level rise and Florida current transport. Ocean Sci 11:607–615. https://doi.org/10.5194/os-11-607-2015
Park K, Federico I, Di Lorenzo E, Ezer T, Cobb KM, Pinardi N, Coppini G (2022) The contribution of hurricane remote ocean forcing to storm surge along the Southeastern U.S. coast. Coastal Eng 173:104098. https://doi.org/10.1016/j.coastaleng.2022.104098
Parris A, Bromirski P, Burkett V, Cayan D, Culver M, Hall J, Horton B, Knuuti K, Moss R, Obeysekera J, Sallenger A, Weiss J (2012) Global sea level rise scenarios for the US National Climate Assessment. NOAA Tech Memo OAR CPO-1, 37 pp. https://scenarios.globalchange.gov/sites/default/files/NOAA_SLR_r3_0.pdf
Sallenger AH, Doran KS, Howd PA (2012) Hotspot of accelerated sea-level rise on the Atlantic coast of North America. Nat Clim Chan 2:884–888. https://doi.org/10.1038/nclimate1597
Sweet W, Park J (2014) From the extreme to the mean: acceleration and tipping points of coastal inundation from sea level rise. Earth's Future 2(12):579–600. https://doi.org/10.1002/2014EF000272
Sweet W, Kopp RE, Weaver CP, Obeysekera J, Horton RM, Thieler ER, Zervas C (2017) Global and regional sea level rise scenarios for the United States. NOAA Technical report NOS CO-OPS 083, NOAA Silver Spring, MD, 64 pp. https://tidesandcurrents.noaa.gov/publications/techrpt83_Global_and_Regional_SLR_Scenarios_for_the_US_final.pdf
Sweet W, Dusek G, Obeysekera J, Marra JJ (2018) Patterns and projections of high tide flooding along the U.S. coastline using a common impact threshold. NOAA Technical report NOS CO-OPS 086, NOAA Silver Spring, MD, 44 pp. https://tidesandcurrents.noaa.gov/publications/techrpt86_PaP_of_HTFlooding.pdf
Sweet W, Hamlington BD, Kopp RE, Weaver CP, Barnard PL, Bekaert D, Brooks W, Craghan M, Dusek G, Frederikse T, Garner G, Genz AS, Krasting JP, Larour E, Marcy D, Marra JJ, Obeysekera J, Osler M, Pendleton M, Roman D, Schmied L, Veatch W, White KD, Zuzak C (2022) Global and regional sea level rise scenarios for the United States: updated mean projections and extreme water level probabilities along U.S. coastlines. NOAA Technical Report NOS 01. National Oceanic and Atmospheric Administration, National Ocean Service, Silver Spring, MD, 111 pp. https://oceanservice.noaa.gov/hazards/sealevelrise/noaa-nos-techrpt01-global-regional-SLR-scenarios-US.pdf
Taherkhani M, Vitousek S, Barnard PL, Frazer N, Anderson TR, Fletcher CH (2020) Sea-level rise exponentially increases coastal flood frequency. Sci Rep 10:6466. https://doi.org/10.1038/s41598-020-62188-4
Thomson RE, Tabata S (1987) Steric height trends at Ocean Station PAPA in the northeast Pacific Ocean. Mar Geod 11(2–3):103–113. https://doi.org/10.1080/15210608709379553
Valle-Levinson A, Dutton A, Martin JB (2017) Spatial and temporal variability of sea level rise hot spots over the eastern United States. Geophys Res Lett 44:7876–7882. https://doi.org/10.1002/2017GL073926
Wdowinski S, Bray R, Kirtman BP, Wu Z (2016) Increasing flooding hazard in coastal communities due to rising sea level: case study of Miami Beach, Florida. Ocean Coast Man 126:1–8. https://doi.org/10.1016/j.ocecoaman.2016.03.002
Wu Z, Huang NE (2009) Ensemble empirical mode decomposition: a noise-assisted data analysis method. Adv Adapt Data Analys 1(1):1–41. https://doi.org/10.1142/S1793536909000047
Wu Z, Huang NE, Long SR, Peng C-K (2007) On the trend, detrending and variability of nonlinear and non-stationary time series. Proc Natl Acad Sci 104:14889–14894. https://doi.org/10.1073/pnas.0701020104